Available online at www.sciencedirect.com
ScienceDirect
Ceramics International 36 (2010) 23–31
CERAMICS INTERNATIONAL
www.elsevier.com/locate/ceramint

In situ synthesis of orange rutile ceramic pigments by non-conventional methods

C. Gargori, S. Cerro, R. Galindo, G. Monrós *

Dpt. of Inorganic and Organic Chemistry, Jaume I University, Av. de Vicent Sos Baynat, s/n. 12071, Castellón, Spain

Received 23 February 2009; received in revised form 24 May 2009; accepted 7 June 2009
Available online 7 July 2009

Abstract

Different precursor-mixtures of orange Cr,Sb-TiO_2 ceramic pigment have been obtained by non-conventional methods (heterogeneous ammonia coprecipitation, urea homogeneous coprecipitation, PECHINI polyester method and an original aqueous–organic coprecipitation method in water–diethylenglycol medium) in order to produce in situ the pigment through the ceramic body firing. The pigmenting performances of powders were appraised in two cases: (a) as ceramic pigment for glazed porcelain stoneware and (b) as ceramic inks for screen printing of porcelain stoneware. Samples were characterised by X-ray Diffraction (XRD), Scanning Electron Microscopy (SEM), Transmission Electron Microscopy (TEM), UV–vis-NIR spectroscopy by diffuse reflectance method, CIE-$L^*a^*b^*$ colour parameters, BET specific surface area and crystallite size measured by the Scherrer method. The colouring performance of raw powders obtained by non-conventional methods in glazed porcelain stoneware improves that of the ceramic samples fired at 1100 °C used as reference. TEM observations indicate nanostructured powders with pigmenting performance depending on factors such as their specific surface area (BET), the crystalline phases detected by XRD (e.g. anatase–rutile presence) and their crystallite size (Scherrer measurements). Ammonia coprecipitated samples, both in water and in water–diethylenglycol medium without surfactant addition, or modified by the addition of sodium dodecyl sulphate as surfactant, stand out by their colouring performance.

Keywords: Sol–gel; Aqueous–organic coprecipitation; Rutile; Ceramic pigment

1. Introduction

The high degree of homogeneity achieved from sol–gel mixtures of alkoxides, alkylalkoxides and soluble salts chemically designed (solvent, catalyst, complexing agents, ...) give versatile cheap thin coatings. After controlled hydrolysis-condensation and drying, sol–gel samples allow to produce high reactive powders (nano-sized powders), which sinter easily producing controlled microstructures [1–3]: acicular shaping for tape casting of ferromagnetic materials, aerogels or 98% porous materials (using supercritical drying of raw mixture), controlled mesoporous microstructure, low temperature sintering materials [4].

The traditional procedure of synthesis of ceramic pigments implies the solid state reaction from oxide precursors followed by milling in order to adjust the optimal particle size: coarse particles produce bad colouration, but too much small particles may be dissolved by the matrix. For new applications in ceramics, such as Ink Jet procedures [5–7], it is necessary to use particles of pigment at the nano-scale. However glazes could easily dissolve nanoparticles obtained by milling or other procedures [8,9]. It is necessary to use a self-generating procedure starting with solved precursors in ink medium or from fine particles that join together into optimal aggregates capable to react [10], when glaze or ceramic matrix will be fired, forming the stable ceramic pigment particles. These micro-sized aggregates are integrated by nanoparticles forming nanostructured materials [11,12].

In order to obtain this kind of solid precursor of pigments, coprecipitation and sol–gel routes have been applied as chemical processes, which improve microstructural characteristics in the preparation of $Cr_{0.015}Sb_{0.015}Ti_{0.97}O_2$ compositions [13] by several coprecipitation methods. Rutile is the most common natural polymorph of TiO_2 because it has the lowest volume of the three polymorphs first described by Vegard in

* Corresponding author. Tel.: +34 964 728250; fax: +34 964 728214.
E-mail address: monros@qio.uji.es (G. Monrós).

0272-8842/$36.00
doi:10.1016/j.ceramint.2009.06.013

1916: rutile, anatase and brookite [14–16]. Rutile shows one of the highest refractive index among the crystalline known phases. Its stability and high refractive index are interesting properties for ceramic pigments. So finely powdered rutile is a brilliant white pigment used in paints, plastics, papers, foods, and other applications that call for a bright white colour. Titanium dioxide pigment is the single greatest use of titanium worldwide [17,18].

Industrial rutile pigments are manufactured using several trivalent chromophores: Cr (giving an orange hue), Mn (tan), Ni (yellow) and V (gray), but for achieving the charge neutrality of the network, a second element or pentavalent counterion (i.e. Mo, Sb, Nb or W) is necessary to be added. The colour of these pigments is determined by both metal–ligand charge transfer ($Ti^{4+} \leftrightarrow O^{2-}$) and crystal field effects (transition metals substituting Ti^{4+} in octahedral coordination) [19–21]. Rutile pigments show thermal limited application for through-body (up to 1250 °C) and glaze applications (up to 1100 °C). The best colouration of porcelain stoneware bodies is achieved with Sb or W as counterions. The best glaze colours are accomplished by W-bearing pigments, but Nb or Sb-containing samples are more stable, except than for the V–W coupling. Usually the precursor of titanium in solid state reactions is anatase which transforms to rutile during the synthesis. The anatase–rutile transition is heavily affected by chromophores with a lowering of the onset temperature: V < Cr < Ni < Mn; the effect of counterions is almost completely hidden by that of chromophores, even if the sequence Mo < Sb < W < Nb may be inferred.

The crystal structure of rutile pigments is modified by chromophores and counterions producing a progressive distortion of the octahedral site and a peculiar variation of the mean Ti–O bond length, with longer basal Ti–O distances and a shorter apical Ti–O distance. The pigment co-doped with V and W is different for its minimum Ti–O bond length distortion, an almost regular TiO_6 octahedron [13].

The unstability of the rutile based pigments in ceramic matrices is the main problem for its use in high temperature applications such as glazes or Ink Jet applications for porcelain stoneware (1200 °C) [22,23]. In effect, the solid solutions obtained are dissolved by glazes at 1200 °C and recrystallise on cooling, but solid solution is lost and colour can be altered. In order to avoid dissolution of pigment, two main possibilities can be proposed: (a) use of relative high size particle pigment which produces a coarse colouration and (b) in situ synthesis of pigment during tile firing (around 60 min of duration with 5 min soaking at maximum temperature at 1200 °C). For this self-generating pigment, it is necessary to design a raw microstructure of aggregate precursors, which in glazes reacts to form the pigment during tile firing.

In this paper a precursor-mixture of orange Cr,Sb-TiO_2 ceramic pigment has been obtained by non-conventional methods. The pigmenting performances of powders were appraised in two cases: (a) as ceramic pigment adding centrifuged powders directly to a porcelain stoneware glaze and deposited by Doctor Blade technique on a porcelain stoneware body and fired following a conventional firing cycle and (b) as ceramic inks for screen printing of the emulsion obtained mixing polyethilenglicol and centrifuged powder powder on porcelain stoneware and fired by a conventional firing cycle. As reference, the pigment was obtained also by solid state reaction from oxide precursors (ceramic method).

2. Experimental

2.1. Synthesis of samples

Rutile samples of composition $Cr_{0.015}Sb_{0.015}Ti_{0.97}O_2$ were prepared by several methods:

(a) Ceramic method (CE), used as colour reference. Both Sb(III) and Sb(V) oxides were used as antimonium precursor in order to optimise valence and temperature of synthesis. In this method, antimonium oxides, chromium (III) oxide and anatase, supplied by Panreac S.A., used as precursors to 20 g of final product, were milled in acetone medium, and fired at 900, 1000 and 1100 °C with 1 h of soaking time.

(b) Heterogeneous ammonia coprecipitation (NH_3–CO). $SbCl_3$ for 10 g of final product was slowly solved in 60 ml of warm 1 M nitric acid solution, then 200 ml of water and $Cr(NO_3)_3{\cdot}9H_2O$ were added maintaining continuous stirring and 70 °C. Then titanium isopropoxyde was dropped and after that, 35% ammonia solution was dropped until pH 8. A finely green coprecipitated suspension was obtained and used as ink by screen printing on porcelain stoneware. Precipitated powder was separated by centrifugation, washed with ethanol and dried in air.

(c) Homogeneous urea coprecipitation method (UREA-CO). Using the same procedure b, urea was added as precipitant agent instead ammonia in a molar ratio urea:Ti = 4:1 and boiled during 1 h in order to reach the homogeneous decomposition of urea into ammonia:

$$(NH_2)_2CO + H_2O \rightarrow CO_2 + 2NH_3 \quad (1)$$

The green precipitate obtained was separated by centrifugation and washed with ethanol.

(d) PECHINI polyester method (PECHINI). Using the same procedure b, citric acid (molar ratio citric acid:Ti = 1:1) was added followed by diethylenglycol (molar ratio diethylenglycol:Ti = 1:1) instead the ammonia addition. Temperature and stirring were maintained during 1 h and the polyester obtained was dried at 110 °C.

Powders obtained in NH_3–CO, UREA-CO and AQ-CO coprecipitation methods were dried in air and used as ceramic pigment in raw form or in thermal stabilised powder at 500 °C. How it has been indicated previously, usually the precursor of titanium in rutile pigments synthesis is anatase, which transforms to rutile during the synthesis. Raw powders obtained from the coprecipitation methods are amorphous or show anatase–rutile crystallisation depending on their homogeneity degree. High homogeneous powders show low tendency to crystallisation because must crystallise by the slow homogeneous nucleation-growth mechanism and

remain amorphous or showing anatase of low crystallite size. In contrast, heterogeneous coprecipitates crystallise by fast heterogeneous nucleation route and show anatase of relative high crystallite size and rutile: consequently react easily to produce the pigmenting solid solution. It is well known that the homogeneity of coprecipitates is higher using organic medium and homogeneous precipitants. Therefore it can be expected that the crystallisation capacity of coprecipitates increases (because the homogeneity degree decreases) in the sequence: NH_3–CO > UREA-CO > PECHINI. In order to improve the reactivity of the NH_3–CO coprecipitation method, aqueous–organic coprecipitation method AQ-CO using surfactant addition has been studied [24,25].

(e) Aqueous–organic coprecipitation method (AQ-CO). In order to obtain an emulsion of fine particles, ammonia coprecipitation was carried out in a water–diethylenglycol medium modified by the addition of a surfactant. $SbCl_3$ for 10 g of final product was slowly added to 60 ml of warm 1 M nitric acid solution until total dissolution and then $Cr(NO_3)_3{\cdot}9H_2O$ was added maintaining continuous stirring at 70 °C. After that 100 ml of diethylenglycol and 0.5 g of surfactant were added until complete solution. During the process continuous stirring was maintained at 70 °C. Then titanium isopropoxyde was dropped and after that ammonia 35% aqueous solution was dropped slowly until pH 8 was attained. Three surfactants were used: alkyldibencilamonium ABA, hexamethyltrimethylamonium HTA and sodium dodecyl sulphate SDS. The surfactant-free and the ABA added samples produced a green viscous emulsion. The HTA and SDS added samples gave a light green and liquid suspension. This suspension was used as ink by screen printing on porcelain stoneware. The precipitated was separated by centrifugation and washed with ethanol.

How it has been indicated, the precipitates have been checked as ceramic inks, using the direct suspension obtained in coprecipitation or the emulsion obtained mixing polyethilenglicol:centrifugated powder = 50:20 wt. ratio which was screen printed on a porcelain stoneware and fired by a conventional tile firing cycle. The thickness of prepared films, using a 48 threads/cm mesh, is of the order of 1 μm.

2.2. Characterisation of samples

X-ray Diffraction (XRD) was carried out on a Siemens D5000 diffractometer using Cu Kα radiation, 20–70° 2θ range, scan rate 0.05° 2θ/s, 10 s per step and 40 kV and 20 mA conditions.

Microstructure characterisation of powders was carried out by Scanning Electron Microscopy (SEM), using a Leo-440i microscope supplied by LEYCA. Likewise SEM-EDXA microstructural analysis was obtained in a LEO-440i electronic microscope equipped by a microanalysis system supplied by Oxford.

Transmission Electron Microscopy (TEM) characterisation was carried out in a Hitachi H600 100 kV which allows obtaining electron patterns by selected area diffraction patterns (SADP).

UV–vis-NIR spectra of 5% weight glazed samples in a conventional SiO_2–CaO–ZnO glaze for porcelain stoneware have been collected using a Lambda 2000 spectrometer supplied by PerkinElmer through diffuse reflectance technique. $L^*a^*b^*$ colour parameters of, glazed samples were measured following the CIE (Commission International de l'Eclairage) colorimetric method [26] using a PerkinElmer spectrophotometer, with standard lighting C. On this method, L^* is a measure of brightness (100 = white, 0 = black) and a^* and b^* of chroma ($-a^*$ = green, $+a^*$ = red, $-b^*$ = blue, $+b^*$ = yellow).

BET [27] specific surface analyser Gemini V equipped with Flow Prep 060 gas desorption system supplied by Micromeritics was used for specific surface measurements of samples.

The crystallite size was measured by the Scherrer method and is given by:

$$D = \frac{K\lambda}{B_{1/2}\cos\Theta_B} \quad (2)$$

where D *is* the average grain size, Θ_B is the Bragg angle, λ is the wavelength of the X-ray and K is a unit cell geometry dependent constant whose value is typically between 0.85 and 0.99. $B_{1/2}$ is the full-width-half-max of the peak after correcting for peak broadening which is caused by the diffractometer using quartz as reference material [12]. The mean crystallite size was calculated from the broadening of the $2\Theta = 25°$ peak of the (1 0 1) diffraction plane for anatase and $2\Theta = 27.5°$ of the (1 1 0) plane for rutile.

3. Results and discussion

3.1. Ceramic route

XRD evolution of crystalline phases in ceramic samples and CIE-$L^*a^*b^*$ of fired powders 5% glazed in a CaO–ZnO–SiO_2 conventional glaze in function of antimonium valence in oxide used as raw material are shown in Table 1 and Fig. 1. The anatase-to-rutile transformation is favoured by Sb(V) oxide; in effect, at 900 °C the synthesised sample using Sb(V) formed rutile and the orange shade of glazed samples is better than for the Sb(III) sample (higher a^* and b^* parameters). However at 1000 and 1100 °C only rutile is detected by XRD analysis in all samples and colour shade of glazed samples are very similar in both Sb(III) and Sb(V) samples: around $L^*a^*b^*$ = 76/12/26.

3.2. Raw samples obtained by non-conventional methods

XRD evolution of crystalline phases in powdered samples and CIE-$L^*a^*b^*$ parameters in 5% glazed in a CaO–ZnO–SiO_2 conventional glaze in function of the non-conventional method are shown in Table 2 and Fig. 2.

In all cases, peaks of low intensity associated to anatase are detected and in the coprecipitated samples NH_3–CO and UREA-CO the presence of rutile is already detected together

Table 1
XRD evolution of crystalline phases in ceramic samples and CIE-$L^*a^*b^*$ of fired powders 5% glazed in a conventional stoneware glaze.

Sample	900 °C/1 h	1000 °C/1 h	1100 °C/1 h
Sb(III)	A(s)R(w) $L^*/a^*/b^*$ = 76/5/22	R(vs) 75/12/24	R(vs) 75/12/24
Sb(V)	R(s)A(m) $L^*/a^*/b^*$ = 78/8/24	R(vs) 78/9/23	R(vs) 76/12/26

Crystalline phases: A (anatase), R (rutile). Intensity of peaks: s (strong), m (medium), w (weak), vs (very strong).

Table 2
XRD evolution of crystalline phases in powdered samples and CIE-$L^*a^*b^*$ parameters in 5% glazed samples on function of the preparation method.

Sample	NH_3–CO	UREA-CO	PECHINI
Raw	A(w)R(vw) $L^*/a^*/b^*$ = 81/9/22	A(vw)N(s) 85/4/22	A(w) 90/0/8
Stabilised 500 °C/1 h	A(m)R(vw) $L^*/a^*/b^*$ = 71/16/26	A(m) 81/10/29	A(m) 88/1/7

Crystalline phases: A (anatase), R (rutile). Intensity of peaks: s (strong), m (medium), w (weak), vw (very weak).

with ammonium chloride. The mean crystallite size calculated for anatase and rutile are shown in Table 3. The crystallite size of anatase in all raw samples increases in the order NH_3–CO > UREA-CO > PECHINI in agreement with the homogeneity degree expected from of the preparation method [24,25]. In this sense, NH_3–CO method stands out by their high crystallite size of anatase detected together rutile. Likewise NH_3–CO sample shows the best orange colour ($L^*/a^*/b^*$ = 81/9/22) comparable to the colour obtained from fired ceramic samples. On the other hand, the homogeneous PECHINI sample shows very weak crystallisation and low crystallite size of anatase, but it does not show pigmenting capacity.

3.3. Stabilised samples obtained by non-conventional methods

In order to eliminate residual organics and ammonium chloride salt from the raw powders obtained by non-conventional methods, powders were submitted to firing at 500 °C with 1 h of soaking time (stabilisation firing). From XRD on Table 2 of stabilised samples at 500 °C can be observed: (a) the XRD peaks of ammonium chloride disappear on firing, (b) the crystallite size of anatase increases on firing in all samples, (c) likewise on the raw samples, the crystallite size of anatase of samples increases in the order NH_3–CO > UREA-

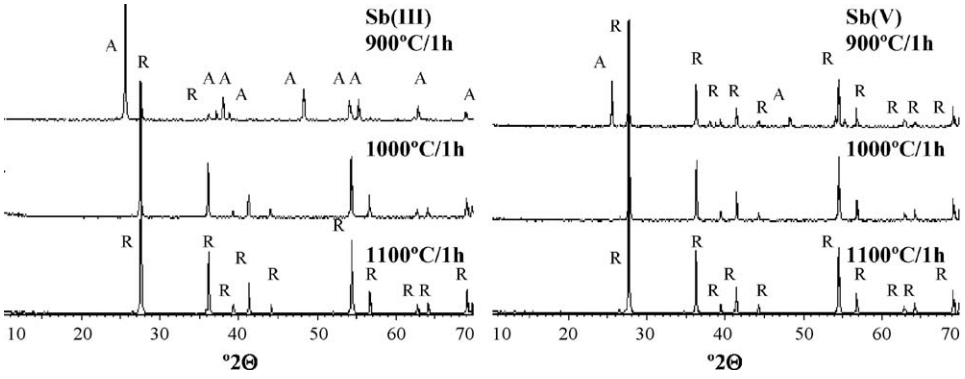

Fig. 1. XRD evolution of CE samples with temperature: A (anatase), R (rutile).

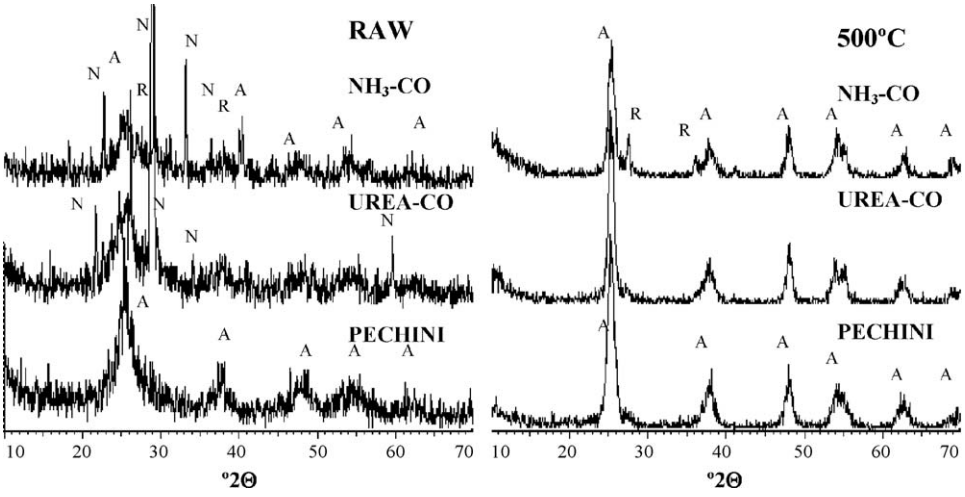

Fig. 2. XRD of samples obtained by indicated methods (raw and fired at 500 °C): A (anatase), R (rutile), N (NH_4Cl).

Table 3
Crystallite size of anatase and rutile detected crystalline phases (Scherrer method).

Sample	T (°C)	Anatase D (nm)	Rutile D (nm)
NH_3–CO	Raw	85	182
	500	226	454
UREA-CO	Raw	82	–
	500	205	–
PECHINI	Raw	80	–
	500	178	–
AQ-CO	Raw-without surfactant	127	80
	Raw-ABA	58	64
	Raw-HTA	–	151
	Raw-SDS	62	64

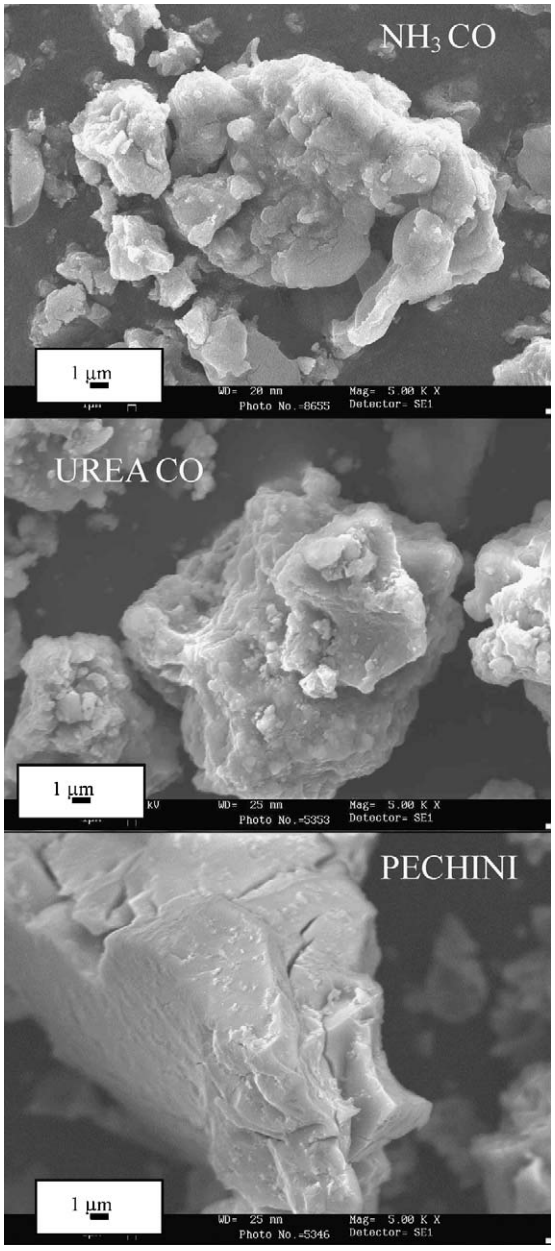

Fig. 3. SEM micrographs of stabilised samples (500 °C/1 h).

Table 4
XRD evolution of crystalline phases in powdered samples and CIE-$L^*a^*b^*$ parameters in glazed samples with 5% of powder addition of AQ-CO samples.

Sample	Raw	Stabilised 500 °C/1 h
Surfactant-free	R,A(w) N(s) $L^*/a^*/b^*$ = 77/13/25	R(m)A(w) 71/13/22
ABA	R,A(w)N(s) $L^*/a^*/b^*$ = 78/12/24	R(w) 73/14/25
HTA	A(w) $L^*/a^*/b^*$ = 80/10/22	R(m) 77/12/29
SDS	R(w)A(w) $L^*/a^*/b^*$ = 76/13/26	R(m) 72/14/31

Crystalline phases: A (anatase), R (rutile), N (NH_4Cl). Intensity of peaks: s (strong), m (medium), w (weak), vw (very weak).

CO > PECHINI, and (d) the crystallite size of rutile in NH_3–CO sample increases on firing.

CIE-$L^*a^*b^*$ colour parameters of glazed samples containing 5% of pigment are strongly dependent on the preparation method. NH_3–CO sample stabilised at 500 °C/1 h presents the best colour results ($L^*a^*b^*$ = 71/16/26). Fired ceramic samples

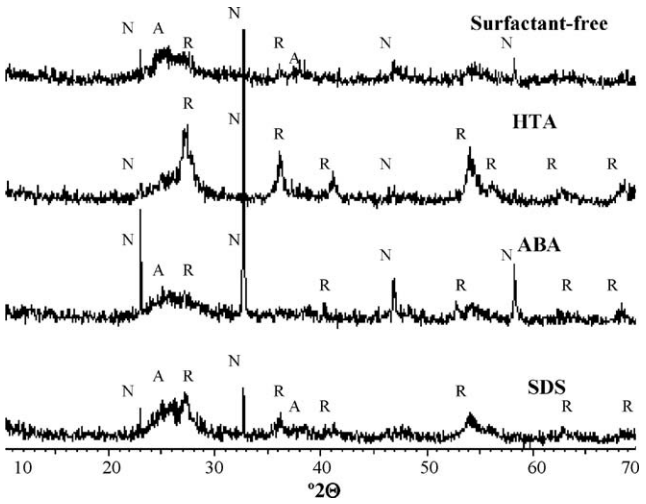

Fig. 4. Evolution of crystalline phases on AQ-CO raw unwashed samples: A (anatase), R (rutile), N (NH_4Cl).

Table 5
BET specific surface area of indicated samples (standard deviations in parentheses).

Sample	m^2/g
CE Sb(III), 1100 °C	2.34(2)
AQ-CO Surfactant-free	52.40(5)
ABA Stabilised 500 °C/1 h	70.0(3)
HTA Stabilised 500 °C/1 h	58.2(2)
SDS Stabilised 500 °C/1 h	84.9(3)

(Table 1) show similar colour to raw NH_3–CO and UREA-CO stabilised samples: brightness parameter L^* in the 75–81 range and red intensity parameter a^* in the 4–12 range. Finally, homogeneous PECHINI method obtained from organic polyester resin precursor shows the worst colour result and the stabilisation treatment does not improve it. These results indicate the high reactivity of non-conventional powders that produce the Cr,Sb-TiO_2 orange colour by in situ synthesis during the glaze firing (only 5 min soaking at maximum temperature 1200 °C) in contrast to ceramic samples, that

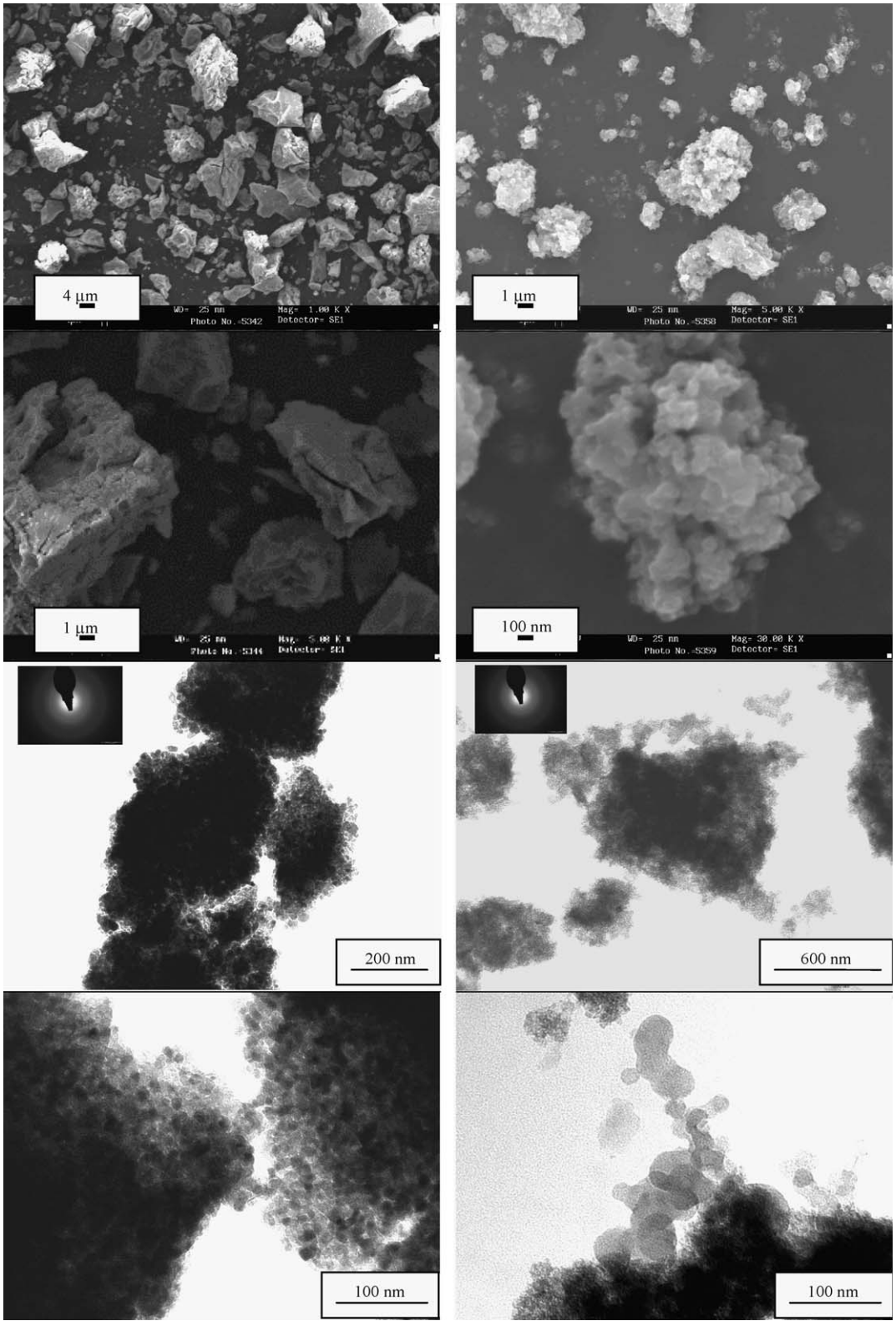

Fig. 5. SEM and TEM micrographs of indicated samples.

previously fired in the range 900–1100 °C, gave a worse orange colour. Likewise, these results are in agreement with the homogeneity degree achieved and crystallisation capacity of the powders [7,24,25]. In this sense, NH_3–CO sample that shows anatase together rutile in raw precipitates reacts easily to produce to Cr,Sb-TiO_2 orange pigment in agreements of the well known fact that anatase-to-rutile transition is necessary in order to reach the solid solution reaction. On the other hand, UREA-CO and PECHINI precipitates, than only show anatase at XRD analysis, did not gave colour on glazed samples containing 5% of powders, the stabilisation treatment improves colour in UREA-CO glazed sample, but not in PECHINI sample.

The microstructure of non-conventional stabilised samples can be observed in the SEM micrographs shown in Figs. 3 and 5. Monolithic grains with a size in the 15–20 μm range can be observed in all cases by SEM microscopy (Fig. 3). However, TEM observations of these grains indicate a nanostructured morphology by aggregation of nanoparticles (Fig. 5).

UV–vis-NIR spectra of coloured glazed samples obtained using non-conventional methods are shown in Fig. 6. The colour of these pigments is determined by both metal–ligand charge transfer ($Ti^{4+} \leftrightarrow O^{2-}$) observed as a sharp band centred at 300 nm and crystal field effects (transition metals substituting Ti^{4+} in octahedral coordination). In the case of Cr^{3+} substitution three main parity-forbidden transitions in octahedral coordination can be seen: $^4A_2(^4F) \rightarrow {}^4T_2(^4F)$ at 570(±10) nm and $^4A_2(^4F) \rightarrow {}^4T_1(^4F)$ at 445(±10) nm, which overlap, and $^4A_2(^4F) \rightarrow {}^4T_2(^4P)$ at 235(±10) nm which overlaps with $Ti^{4+} \leftrightarrow O^{2-}$ band transfer. Two weak Cr^{3+} spin-forbidden transitions ($^4A_2(^4F) \rightarrow {}^2T_1(^2G)$ and $^4A_2(^4F) \rightarrow {}^2E(^2G)$ that overlaps in the 735–740(±10) nm range are observed [13,21]. It can be seen that NH_3–CO stabilised at 500 °C sample, shows the higher absorbance in the 400–600 nm range producing the best orange shade. On the other hand, glazed samples of raw powders show significant absorbance (lower than stabilised samples), and produce in situ pigment performance.

3.4. Samples obtained by aqueous–organic coprecipitation

In order to improve the reactivity of the NH_3–CO coprecipitation method, aqueous–organic coprecipitation method (AQ-CO) using surfactant addition has been studied. The XRD diffractogrammes of powders and CIE-$L^*a^*b^*$ parameters of glazed samples containing 5% of pigment for the AQ-CO samples are shown in Table 4 and Fig. 4. The mean crystallite size for anatase and rutile in these samples is shown in Table 3.

Raw HTA added sample show rutile as the only crystallised phase on Fig. 4 and in the other raw AQ-CO samples anatase together rutile phases are detected. When samples were stabilised at 500 °C, rutile becomes the only crystalline phase detected in all cases. The colour developed by raw washed samples in glaze is similar for all samples (L^* = 76–77 a^* = 12–13) except for the HTA sample that has the poorest colour (L^* = 80 and a^* = 10). On the other hand, all samples stabilised at 500 °C developed more intense colour with L^* = 71–75 and increasing red shade (a^* = 13–14) in comparison with unfired samples. The SDS added sample shows the best orange shade among the samples fired at 500 °C (higher red and yellow shades: a^* = 14 and b^* = 31 respectively).

The specific surface of AQ-CO fired and glazed samples is shown in Table 5 compared with a ceramic CE sample. The higher specific surface is associated to the relatively best pigmenting sample (84.9 m^2/g for SDS added sample), but all samples show similar specific surfaces and higher than ceramic sample used as reference. Likewise surfactant added samples show higher specific surface area than surfactant-free sample. The microstructure of representative AQ-CO samples is displayed on Fig. 5. Raw AQ-CO samples, such as SDS surfactant addition sample in Fig. 5, show monolithic grains of relatively low size at SEM observations (in the 2–10 μm range of diameter), but these grains appear nanostructured at TEM observation (nanoparticles around 10 nm of size). On the other hand, samples stabilised at 500 °C, such as surfactant-free sample in Fig. 5, show sintered aggregates in the 10–30 μm range. The aggregates show a nanostructured appearance at TEM observations with nanoparticle size around 20 nm (in Fig. 5 other spherical higher sized particles associated to residual dried organic surfactant can be observed). In all cases, the aggregates show low crystallisation as indicate electron patterns by selected area diffraction patterns in Fig. 5. The particle size measured by TEM observations is lower than the crystallite size of anatase or rutile crystalline phase measured by XRD Scherrer method. Anatase–rutile crystallisations are not detected by TEM observations, due to the low concentration of crystallites immersed on the amorphous phase observed by TEM.

3.5. Samples used as screen printing inks

Finally, samples have been checked as ceramic inks for screen printing of porcelain stoneware as previously described. The CIE-$L^*a^*b^*$ results obtained in screen printed porcelain stoneware are shown in Table 6 for NH_3–CO and AQ-CO (without surfactant addition) samples. Direct suspensions produce low orange shades (L^* = 83, a^* = 3) due to low concentration of pigment (3 wt.%), but using a sufficient mass of pigment in the ink, when a mixture polyethilenglicol:centrifugated powder = 50:20 wt. ratio is used (around 25 wt.% of pigment in the emulsion), orange colour become more intense than in their homologous glazed samples, reaching a^* = 18 in the AQO-CO (surfactant-free sample). The UV–vis-NIR spectrum

Table 6
Screen printed (48 threads/cm) inks fired under porcelain stoneware.

Sample	Screen printing deposition	$L^*a^*b^*$
NH_3–CO	Coprecipitated suspension	85/3/20
NH_3–CO	Polyethilenglicol:centrifugated powder in a weight ratio of 50:20	77/13/38
AQ-CO surfactant-free	Coprecipitated suspension	86/3/16
AQ-CO surfactant-free	Polyethilenglicol:centrifugated powder in a weight ratio of 50:20	74/18/41

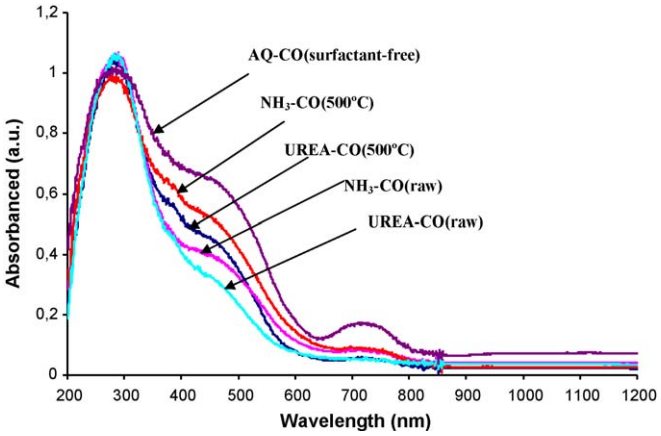

Fig. 6. UV–vis-NIR spectra of indicated samples.

of this sample is shown in Fig. 6. The feature of the spectrum is similar to the glazed samples but the absorbance level of bands due the Cr^{3+} substitution in the rutile network are more intense on the screen printed sample spectrum.

4. Conclusions

Different precursor-mixtures of orange Cr,Sb-TiO_2 ceramic pigment have been obtained by non-conventional methods in order to produce in situ the pigment through the ceramic body firing. The pigmenting performances of powders were appraised as ceramic pigment added to glazed porcelain stoneware and as ceramic inks for screen printing of porcelain stoneware. From the above discussion, the following conclusions stand out:

(1) In the ceramic samples, used as reference, anatase-to-rutile transformation is favoured by Sb(V) oxide (showing rutile since 900 °C), and the orange shade of glazed samples is better than for Sb(III) sample (higher a^* and b^* parameters). However at 1000 and 1100 °C only rutile is detected by XRD analysis in all samples and colour shade of glazed samples is similar in both Sb(III) and Sb(V) samples ($L^*a^*b^* \approx 76/12/26$).

(2) Using non-conventional methods (heterogeneous ammonia coprecipitation, urea homogeneous coprecipitation, PECHINI polyester method and an original aqueous–organic coprecipitation method in water–diethylenglycol medium), high reactivity of raw washed dried powders added to a conventional tile glaze is observed because produce the Cr,Sb-TiO_2 orange colour by in situ synthesis during the glaze firing (only 5 min soaking at maximum temperature 1200 °C), in contrast to ceramic samples, that previously fired in the range 900–1100 °C, gave a worse orange colour. Likewise, these results are in agreement with the homogeneity degree of samples and their resulting crystallisation capacity on the powders (e.g. the NH_3–CO heterogeneous sample, that shows anatase together rutile in raw precipitates, reacts easily to produce Cr,Sb-TiO_2 orange pigment, on the other hand, the homogeneous UREA-CO and PECHINI precipitates, than only show anatase at XRD analysis, did not gave colour on glazed samples containing 5% of powders).

(3) When powders obtained by non-conventional methods were thermal stabilised by firing at 500 °C, the capacity of powders in order to produce Cr,Sb-TiO_2 orange colour by in situ synthesis improves.

(4) The reactivity of the NH_3–CO sample can be improved by the aqueous–organic coprecipitation method AQ-CO using surfactant addition and the colour developed by raw washed samples on glazes is similar for all samples ($L^* = 76$–77, $a^* = 12$–13), except for HTA (hexamethyltrimethylamonium) added sample, that produces the poorest colour, in agreement with the only detection of rutile in raw powders. On the other hand, all samples stabilised at 500 °C developed more intense colour with $L^* = 71$–75 and increasing red shade ($a^* = 13$–14) in comparison with raw samples. The SDS (sodium dodecyl sulphate) added sample shows the best orange shade among the samples fired at 500 °C (higher red and yellow shades: $a^* = 14$ and $b^* = 31$ respectively).

(5) SEM observations indicate monolithic grains of relatively low size (in the 2–10 μm range of diameter), and these grains appear nanostructured at TEM observations (around 10 nm of particle size in raw coprecipitates and 20 nm in samples stabilised at 500 °C). On the other hand, aggregates of samples stabilised at 500 °C, show low crystallisation as indicate electron patterns by selected area diffraction patterns.

(6) Samples checked as ceramic inks by screen printing of the direct suspension of coprecipitates produce weak orange shades ($L^* = 83$, $a^* = 3$) due to low concentration of pigment (3 wt.%), but using sufficiently mass of pigments in the ink, when a mixture polyethilenglicol:centrifugated powder is used (around 25 wt.% of pigment in the emulsion), orange colour is more intense, reaching $a^* = 18$ in the AQO-CO (without surfactant addition) sample.

Acknowledgements

Authors acknowledge the financial support given by MCYT, MAT 2005-0057 project and by FUNDACION CAJA CASTELLÓN, P1-1B2005-06 project.

References

[1] C.J. Brinker, G.W. Scherer, Sol-gel Science: The Physics and Chemistry of Sol-Gel Processing, Academic Press, Inc., San Diego, 1990.
[2] P.A. Lessing, Mixed-cation oxide powders via polymeric precursors, Ceram. Bull. 68 (5) (1989) 1002–1007.
[3] G. Monrós, M.A. Tena, P. Escribano, V. Cantavella, J. Carda, Classical ceramic colors through colloidal and from alkoxides gels, J. Sol-Gel Sci. Technol. 2 (1994) 377–380.
[4] A. Swiderska-Sroda, G. Kalisz, B. Palosz, N. Herlin-Boime, SiC nanoceramics sintered under high pressure, Rev. Mater. Adv. Sci. 18 (2008) 422–424.
[5] G. Monrós, J.A. Badenes, A. García, M.A. Tena, El Color de la Cerámica, Pub. Universitat Jaume I, Spain, 2003.

[6] C. Feldman, Preparation of nanoscale pigment particles, Adv. Mater. 3 (2001) 1301–1303.
[7] C. Feldman, H.O. Jungk, Polyol-mediated preparation of nanoscale oxide particles, Angew. Chem. Int. (2001) 359–362.
[8] G. Baldi. M. Bitossi, A. Barzanti, Ceramic colorants in the form of nanometric suspensions, US patent 7,316,741 B2.
[9] P.M.T. Cavalcante, M. Dondi, G. Guarini, M. Raimondo, G. Baldi, Colour performance of ceramic nano-pigments, Dyes Pigments 80 (2009) 226–232.
[10] J.H. Werth, M. Linsenbhler, S.M. Dammer, Z. Farkas, H. Hinrichsen, K.E. Wirth, D.E. Wolf, Agglomeration of charged nanopowders in suspensions, Powder Technol. 133 (2003) 106–112.
[11] M. Cain, R. Morrel, Nanostructured ceramics. A review or their potential, Appl. Organometall. Chem. 15 (2001) 321–330.
[12] E. Schafler, M. Zehetbauer, Characterization of nanostructured materials by X-ray line profile analysis, Rev. Adv. Mater. Sci. 10 (2005) 28–33.
[13] (a) F. Matteucci, G. Cruciani, M. Dondi, M. Raimondo, The role of counterions (Mo, Nb, Sb, W) in Cr-, Mn-, Ni- and V-doped rutile ceramic pigments Part 1. Crystal structure and phase transformations, Ceram. Int. 32 (4) (2006) 385–392;
(b) M. Dondi, G. Cruciani, G. Guarini, F. Matteucci, M. Raimondo, The role of counterions (Mo, Nb, Sb, W) in Cr-, Mn-, Ni- and V-doped rutile ceramic pigments Part 2. Colour and technological properties, Ceram. Int., 32 (4) (2006) 393–405.
[14] C.J. Harbert, Less familiar elements in ceramic pigments, Ind. Eng. Chem. 30 (7) (1938) 770–772.
[15] S. Cassaignon, M. Koelsch, J.P. Jolivet, Selective synthesis of brookite, anatase and rutile nanoparticles: thermolysis of $TiCl_4$ in aqueous nitric acid, J. Mater. Sci. 42 (16) (2007) 6689–6695.
[16] M. Andersson, L. Österlund, S. Ljungström, A. Palmqvist, Preparation of nanosize anatase and rutile TiO_2 by hydrothermal treatment of microemulsions and their activity for photocatalytic wet oxidation of phenol, J. Phys. Chem. 106 (41) (2002) 10674–10679.
[17] U. Diebold, The surface science of titanium dioxide, Surf. Sci. Rep. 48 (2002) 53–229.
[18] R.F. De Farias, C.C. Guedes, E. Silva, T.G. Restivo, Thermal study of the anatase-rutile structural transitions in sol–gel synthesized titanium dioxide powders, J. Serb. Chem. Soc. 70 (4) (2005) 675–679.
[19] S. Sorlí, M.A. Tena, J.A. Badenes, J. Calbo, M. Llusar, G. Monrós, Structure of $Ni_xA_{1-3x}B_{2x}O_2$(A = Ti,Sn;B = Sb,Nb) solid solutions, J. Eur. Ceram. Soc. 24 (2004) 2425–2432.
[20] M.A. Tena, A. Mestre, A. Garcia, S. Sorli, G. Monros, Synthesis of gray ceramic pigments with rutile structure from alkoxides, J. Sol-gel Sci. Technol. 26 (1–3) (2003) 813–816.
[21] (a) S. Ishida, M. Hayashi, Y. Fujimura, K. Fujiyoshi, Spectroscopic study of the chemical state and coloration of chromium in rutile, J. Am. Ceram. Soc. 73 (11) (1990) 3351–3355;
(b) A.B. Lever, Studies in Physical and Theoretical Chemistry Inorganic Electronic Spectroscopy, vol. 3, Elsevier, Amsterdam, 1986.
[22] D.R. Eppler, R.A. Eppler, The relative stability of ceramic pigments, in: 98th Annual Meeting and the Ceramic Manufacturing Council's Workshop and Exposition: Materials & Equipment/Whitewares: Ceramic Engineering and Science Proceedings, vol. 18 (2), 2008.
[23] R.A. Eppler, Selecting ceramic pigments, in: Materials & Equipment/Whitewares: Ceramic Engineering and Science Proceedings, vol. 8 (11/12), 2008.
[24] P. Shyama, Mukherjee, Homogeneity of gels and gel-derived glasses, J. Non-Cryst. Solids 63 (1–2) (1984) 35–43.
[25] A. García, M. Llusar, J. Badenes, M.A. Tena, G. Monrós, Encapsulation of hematite in zircon by microemulsion and sol-gel methods, J. Sol-gel Technol. 27 (3) (2003) 267–276.
[26] CIE Comission International de l'Eclairage, Recommendations on Uniform Color Spaces, Color Difference Equations, Psychometrics Color Terms. Suplement no. 2 of CIE Pub. No.15 (E1-1.31) 1971, Bureau Central de la CIE, Paris, 1978.
[27] S. Brunauer, P.H. Emmett, E. Teller, Adsorption of gases in multimolecular layers, J. Am. Chem. Soc. 60 (1938) 309–319.